International Journal of Modern Communication Technologies & Research (IJMCTR)
ISSN: 2321-0850, Volume-2, Issue-4, April 2014

Absorption Coefficient of Quantum Well Photodetector for Interband Transition

Soma Ghosh, Piyali Laha, Arpan Deyasi, Ivy Bose, Moulisha Das Burman

***Abstract*— Absorption coefficient of quantum well photodetector is analytically computed as function of operating wavelength for when interband transition is taking place between lowest two states of conduction band and highest two states of valence band respectively. Transition energies are calculated by solving time-independent Schrödinger's equation subject to appropriate boundary conditions for determination of eigenstates, and corresponding absorbance is calculated considering Lorentzian lineshape function. Results show the variation of peak position and also the magnitude of peak by tuning the structural parameters for a particular transition, and the coefficient is also varied for a particular well dimension when different transitions are considered. It is observed that with increase of eigenvalue, magnitude of peak reduces, and blueshift is observed. Separation between the peaks also depends on the well width for different band-to-band transitions. Result is important for designing quantum well based photodetector.**

***Index Terms*— Absorption coefficient, Quantum well, Interband transition, Oscillator strength, Lorentzian lineshape**

I. INTRODUCTION

Quantum well photodetector replaced the conventional optical detector due to its higher quantum efficiency and lower dark current. Simultaneously the demand for THz devices are also increasing due to its nonlinear property [1-2]. Hence researchers designed the quantum well detector in higher frequency region where the advantage of interband transition is considered for moderate bandgap semiconductors instead of conventional design based on intersubband transition [3]. THz quantum optical transmitters [4] and receivers [5] are designed for different material composition, and tuning of structural parameters and choice of quantized energy levels play key role for performance. In this context, study of absorption coefficient is very important for analyzing the optical property of the device.

Dependence of absorption on structural parameters, applied filed, temperature is computed a decade ago [7] for quantum well structure, and is also calculated for coupled quantum dot [8] considering the strain effect when intersubband optical transition is considered. Later, exciton absorption spectra of MQW structure is calculated, and result is used to design electroabsorption modulator [9]. Thermally detected optical absorption and photoluminescence experiments [10] were carried out on MQW structures grown by MBE technique. Review work is carried out for its possible performance as QWIP [11]. Absorption coefficient is tuned by applying reverse bias [12] in quantum modulator for its possible application as electroabsorption modulator. Intersubband optical absorption coefficient is also calculated for MQW structure for lowest two levels under external electric field, and dependences of the coefficient on the applied field [13], barrier thickness and doping concentration are investigated. For MQW structure, and conversion efficiency is increased based on the calculated absorption coefficient [14]. Lal etc. calculated absorption coefficient is calculted for QWIP, and different optical parameters are estimated [15]. It is also measured at 1.3 μm in Ge/SiGe multiple quantum well on Si [16]. The result is useful in designing MQW based solar cell [17]. It is computed for asymmetric MQW structure also for infrared detector application [18]. Absorption coefficient is analytically calculated for weak electromagnetic wave [19] inside cylindrical quantum wire considering electron-optical scattering.

In this paper, absorption coefficient of quantum well is calculated for interband transition energy where highest two states in valence band and lowest two states of conduction band are considered. Lorentzian lineshape function is taken into account for realistic calculation, and structural parameters are tuned to observe the blueshift/redshift of absorbance. Peak of the graph is also noted in this case. Results are suitable for designing THz range quantum well photodetector.

II. MATHEMATICAL MODELING

Optical absorption coefficient for quantum well can be written as

$$\alpha(\omega) = \frac{q^2 m^*}{2\varepsilon_0 \varepsilon_r c n_r \hbar L m_0^2} \frac{P^2}{\hbar\omega} \times \sum_{n,m} \left\langle g_v^m \middle| g_c^n \right\rangle \Theta(E_{mn} - \hbar\omega) \quad (1)$$

where $\left\langle g_v^m \middle| g_c^n \right\rangle$ is the overlap integral between z-dependent envelope functions of conduction band and valence band, L is the width of quantum well, Θ is the Heavyside step function, n_r is the refractive index of the well material, and '*P*' is defined as

Manuscript received April 20, 2014

Soma Ghosh, Department of Electronics & Communication Engineering, RCC Institute of Information Technology, Kolkata, INDIA,
Piyali Laha, Department of Electronics & Communication Engineering, RCC Institute of Information Technology, Kolkata, INDIA,
Arpan Deyasi, Department of Electronics & Communication Engineering, RCC Institute of Information Technology, Kolkata, INDIA,
Ivy Bose, Department of Electronics & Communication Engineering, RCC Institute of Information Technology, Kolkata, INDIA,
Moulisha Das Burman, Department of Electronics & Communication Engineering, RCC Institute of Information Technology, Kolkata, INDIA,

$$P = N\int_{cell} \psi_{k_c}^{*}(\vec{r}')\, p_A\, \psi_{k_v}(\vec{r}')\, d^3r' \tag{2}$$

The overlap integral defined in eq (1) provides the selection rule for transition. It may be written as

$$\left\langle g_v^{\,m} \middle| g_c^{\,n} \right\rangle = \delta_{k,k'} \int_{-L/2}^{L/2} \chi_m^{\,h}(z)\, \chi_n^{\,e}(z)\, dz \tag{3}$$

For quantum well,

$$\chi_n(z) = \sqrt{\frac{2}{L}} \cos\left(\frac{n\pi z}{L}\right) \tag{4.1}$$

for odd '*n*'

$$\chi_n(z) = \sqrt{\frac{2}{L}} \sin\left(\frac{n\pi z}{L}\right) \tag{4.2}$$

for even '*n*'

Hence, Eq (1) may be modified as

$$\alpha(\omega) = \frac{2\pi q^2 \hbar}{\varepsilon_0 \varepsilon_r c n_r m^{*2} V} \frac{1}{\hbar\omega} \times \sum_{i,j} \left|\langle i|p_z|j\rangle\right|^2 \delta(E_j - E_i - \hbar\omega)(f_{FD}^{\,i} - f_{FD}^{\,j}) \tag{5}$$

where '*i*' and '*j*' are the initial and final states, and f_{FD} is the Fermi-Dirac distribution function. The factor 2 is added for spin degeneracy, and the δ function is introduced to conserve the momentum.

For two consecutive states, Eq. (5) may be written as

$$\alpha(\omega) = \frac{2\pi q^2 \hbar}{\varepsilon_0 \varepsilon_r c n_r m^{*2} V} \frac{1}{\hbar\omega} \left[\frac{8\hbar}{3L}\right]^2 \times \sum_{i,j} \delta(E_j - E_i - \hbar\omega)(f_{FD}^{\,i} - f_{FD}^{\,j}) \tag{6}$$

If the quantum well is doped and Fermi energy level is above the ground state and first excited state is completely empty, then

$$\alpha(\omega) = \frac{n_s \pi q^2 \hbar}{\varepsilon_0 \varepsilon_r c n_r m^{*2} L} \frac{1}{\hbar\omega} \left[\frac{8\hbar}{3L}\right]^2 \delta(\Delta E - \hbar\omega) \tag{7}$$

where n_s is sheet charge density. Defining oscillator strength between 1st state to 2nd state as

$$f_{21} = \frac{2}{m^* \hbar\omega} \left[\frac{8\hbar}{3L}\right]^2 \tag{8}$$

Eq. (7) can be put into the form

$$\alpha(\omega) = \frac{n_s \pi q^2 \hbar}{2\varepsilon_0 \varepsilon_r c n_r m^* L} f_{21} \delta(\Delta E - \hbar\omega) \tag{9}$$

Experimental work shows the broadening of peaks, which can be theoretically obtained by introducing Lorentzian lineshape function replacing the ideal delta function. Hence final expression of absorption coefficient may be written as

$$\alpha(\omega) = \frac{n_s \pi q^2 \hbar}{2\varepsilon_0 \varepsilon_r c n_r m^* L} f_{21} \frac{\Gamma}{\pi\left[(\hbar\omega - \Delta E)^2 + \Gamma^2\right]} \tag{10}$$

where Γ is half-width at half of the maximum.

III. Results & Discussion

Using Eq. (10), absorption coefficient is calculated as a function of operating wavelength for different well width, as shown in Fig 1. For lower well dimension, it is found that the difference in peak position for transition to the ground level of conduction band from the highest two valence band states are very close, and is true when first excited level of conduction band is considered also. This is depicted in Fig 1a.

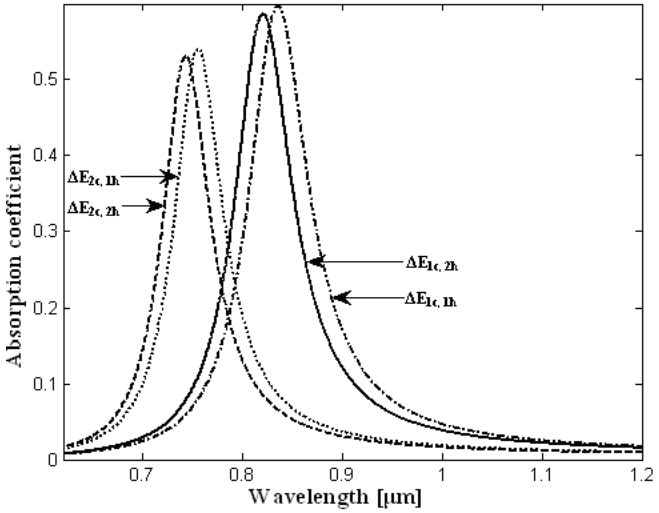

Fig 1a: Absorption coefficient profile with wavelength for different interband transition energies when well width is 7 nm

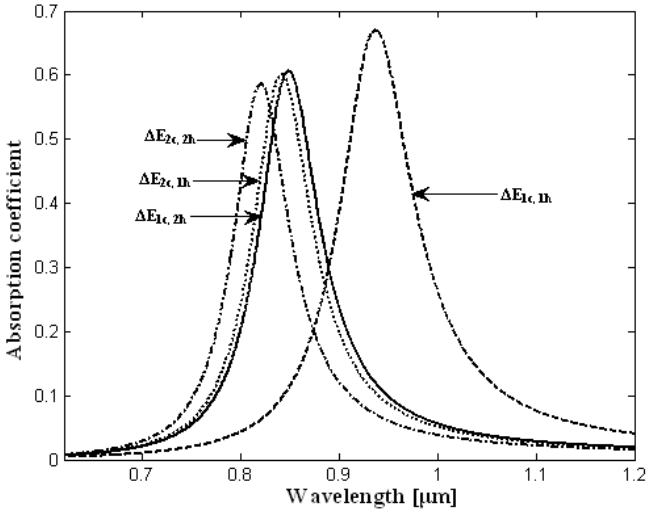

Fig 1b: Absorption coefficient profile with wavelength for different interband transition energies when well width is 15 nm

Again, when the energy difference between the bands increases, interband transition energy naturally increases. This reduces the peak of absorbance amplitude, provided half-width at half-maximum is kept constant throughout the simulation. With increase of well dimension, redshift is observed for all the profiles corresponding to the transition energies. Also the wavelength separation between the transitions for same state of conduction band from different states of valence bands increases. Peak value of the absorption coefficients also increase for all the cases, shown in Fig 1b.

Fig 2 shows the absorption coefficient with wavelength for different well widths when interband transition is calculated from the highest state of valence band. From the plot, it may be seen that with reduction of well dimension, blueshift is observed. Peak of absorbance also decreases with higher well

width which is because of the following reason: Reduction of well width increases quantum confinement which increases the eigenenergies in conduction band and reduces in valence band. This increases transition energies. Higher transition energy makes blueshift of absorbance profile along with reduction of peak magnitude. In Fig 2a, results are plotted for transitions to the ground state of conduction band, whereas in Fig 2b, plots are made for the transitions to the first excited state of conduction band. A comparative study shows that redshift is observed when lower state of conduction band is considered. Also closeness of the plots increases in Fig 2b due to higher transition energy.

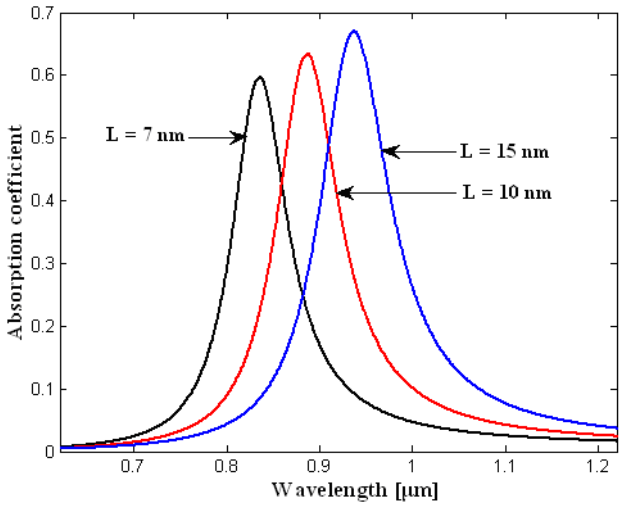

Fig 2a: Absorption coefficient profile with wavelength for different well widths when transition is taking place from highest state of valence band to ground state of conduction band

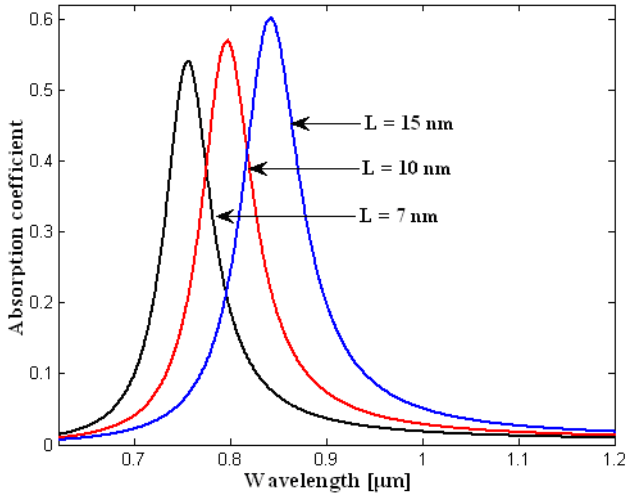

Fig 2b: Absorption coefficient profile with wavelength for different well widths when transition is taking place from highest state of valence band to the first excited state of conduction band

Fig 3 shows the absorption coefficient with wavelength for different well widths when interband transition is calculated from the second highest state of valence band. It is observed from Fig 3a that as the transition energy is almost equal for 10 nm and 15 nm well width for this case, so the peaks appear very close. Also from the plot, it may be concluded that variation of peak magnitude is almost negligible due to the almost equal magnitude of transition energy. In Fig 3b, again variation is distinguishable due to the position of first excited state in conduction band. But for all the four cases (Fig 2 and Fig 3), blueshift is observed with increase of transition energy. Hence suitable tailoring of absorption coefficient is possible by appropriate choice of well width and transition states in valence and conduction bands.

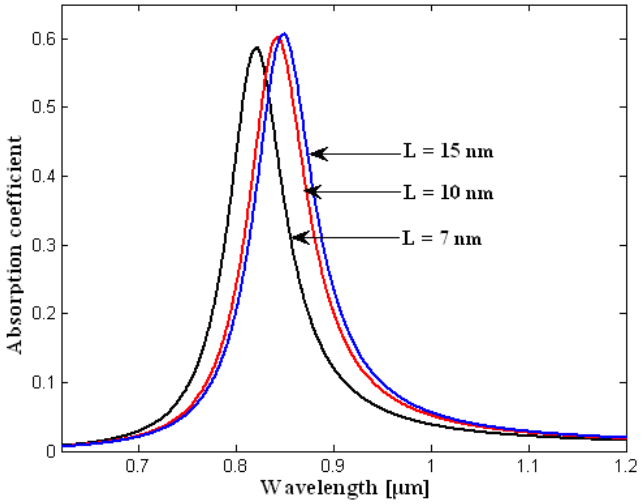

Fig 3a: Absorption coefficient profile with wavelength for different well widths when transition is taking place from second highest state of valence band to ground state of conduction band

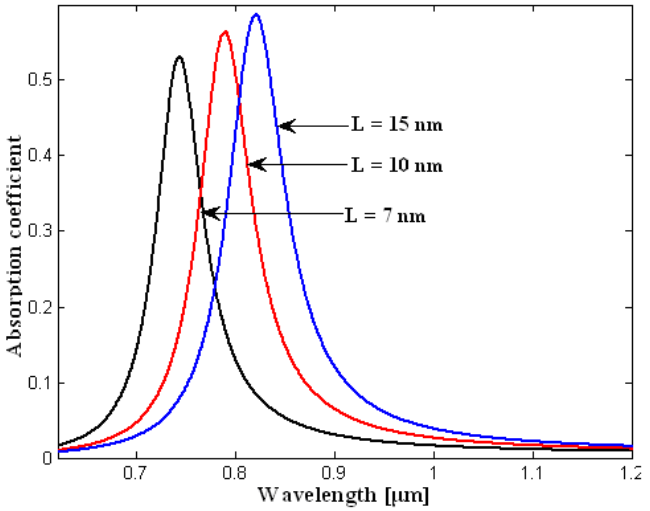

Fig 3b: Absorption coefficient profile with wavelength for different well widths when transition is taking place from second highest state of valence band to the first excited state of conduction band

IV. Conclusion

Absorption coefficient of single rectangular quantum well structure is computed considering Lorentzian lineshape function for different well dimensions. Interband transition energy is calculated between lowest two states of conduction band and highest two states of valence band, and corresponding absorbance is plotted as a function of operating wavelength. Redshift/ blueshift are observed by tuning the structural parameters, and also by considering the different band-to-band transitions. Result is significant for design of quantum well based photodetector.

References

[1] G. Rezaei, Z. Mousazadeh, and B. Vaseghi, "Nonlinear optical properties of a two-dimensional elliptic quantum dot," Physica E: Low-dimensional Systems and Nanostructures, vol. 42(5), pp. 1477–1481, 2010.

[2] X. L. Cao et al., "THz-wave difference frequency generation by phase matching in GaAs/AlxGa1−xAs asymmetric quantum well," Chin. Phys. Lett. 29(1), 014207 (2012).

[3] E. Ozturkl, H. Saril, and I. Sokmen, "Intersubband optical absorption in double quantum well under intense laser field," Eur. Phys. J. Appl. Phys. 35(01), 1–5 (2006).

[4] C. H. Yu et al., "Strong enhancement of terahertz response in GaAs⁄AlGaAs quantum well photodetector by magnetic field," Appl. Phys. Lett. 97(2), 022102 (2010).

[5] S. Kalchmair et al., "Photonic crystal slab quantum well infrared photodetector," Appl. Phys. Lett. 98(1), 011105 (2011).

[6] R. K. Lal, B. Gupt, M. Das, "Proposed generalized numerical model for energy sub-band calculation of quantum well photodetectors", Proceedings of Photonics, p. 352, Dec 2010.

[7] S. Zivanovic, V. Milanovic, Z. Ikonic, "Intraband absorption in semiconductor quantum wells in the presence of a perpendicular magnetic field", Physical review B, vol. 52, 8305-8311, 1995.

[8] S. S. Li, J. B. Xia, "Intraband optical absorption in semiconductor coupled quantum dots", Physical review B, vol. 55, pp. 15434-15437, 1997.

[9] Z. B. Hao, C. L. Guo, W. Y. Zhang, Y. Luo, "Theoretical Analysis of InGaAsP/InGaAsP Multiple-Quantum-Wells Electroabsorption Modulators for the Application of High-Speed Low Driving Voltage Integrated Light Source", Journal of the Korean Physical Society, vol. 34, pp. S104-S108, 1999.

[10] J. Kvietkova, L. Siozade, P. Disseix, A. Vasson, J. Leymarie, B. Damilano, N. Grandjean and J. Massies, "Optical Investigations and Absorption Coefficient Determination of InGaN/GaN Quantum Wells", volume 190, pp 135-140, 2002.

[11] A. Rogalski, "Quantum well photoconductors in infrared detector technology", Journal of Applied Physics, vol. 93, pp. 4355-4391, 2003.

[12] I. Friel, C. Thomidis, and T. D. Moustakasa, "Ultraviolet electroabsorption modulator based on AlGaN/GaN multiple quantum wells", Journal of Applied Physics, vol. 97, p. 123515, 2005.

[13] N. Sfina, S. A. B. Nasrallah, S. Mnasri and M. Said, "Absorption coefficient of intersubband transition at 1.55 μm in (CdS/ZnSe)/BeTe quantum wells", Journal of Physics D: Applied Physics vol. 42, p. 045101, 2009.

[14] P. Sterian, S. Fara, L. Fara, M. Iancu, "A Study of The Optical Properties of Quantum Well Solar Cells aimed at Optimizing their Configuration", U.P.B. Sci . Bull., Series A, Vol. 72, pp. 9-20, 2010.

[15] T K Parashar, R K Pal, "Modeling of gaAs/Al0.2Ga0.8As quantum well gas detector for LWIR region", MIT International Journal of Electronics and Communication Engineering, vol 1, no 2, pp. 97-100, 2011.

[16] L. Lever, Y. Hu, M. Myronov, X. Liu, N. Owens, F. Y. Gardes, I. P. Marko, S. J. Sweeney, Z. Ikonić, D. R. Leadley, G. T. Reed, and R. W. Kelsall, "Modulation of the absorption coefficient at 1.3 μm in Ge/SiGe multiple quantum well heterostructures on silicon", Optics Letters, vol. 36, pp. 4158-4160, 2011.

[17] S. Fara, P. Sterian, L. Fara, M. Iancu, and A. Sterian, "New Results in Optical Modeling of Quantum Well Solar Cells", International Journal of Photoenergy, Article ID 810801, doi:10.1155/2012/810801, 2012.

[18] X. L. Cao, J. Q. Yao, K. Zhong, D. G. Xu, "Intersubband absorption properties of GaAs⁄$Al_xGa_{1-x}As$ asymmetric quantum well based on optical difference frequency", Optical Engineering, vol. 52(1), p. 014001, 2013.

[19] N. T. T. Nhan, N. V. Nhan, "Calculation Absorption Coefficient of a Weak Electromagnetic Wave by Confined Electrons in Cylindrical Quantum Wires in the Presence of Laser Radiation by Using the Quantum Kinetic Equation", Progress in Electromagnetics Research M, vol. 34, pp. 47-54, 2014